ACS OMEGA

Open Access

http://pubs.acs.org/journal/acsodf

Article

Effective Treatment Methodology for Environmental Safeguard Catalytic Degradation of Fluconazole by Permanganate Ions in Different Acidic Environments: Kinetics, Mechanistics, RSM, and DFT Modeling

Arafat Toghan,* Ahmed Fawzy,* Nada Alqarni, Ahmed M. Eldesoky, Omar K. Alduaij, and Ahmed A. Farag*

Cite This: *ACS Omega* 2024, 9, 10190−10200

Read Online

ACCESS | Metrics & More | Article Recommendations | Supporting Information

ABSTRACT: In this paper, the degradation of fluconazole drug (Flz) was explored kinetically utilizing permanganate ion [MnO_4^-] as an oxidant in different acidic environments, namely sulfuric and perchloric acids at various temperatures. Stoichiometry of the reactions between Flz and [MnO_4^-] in both acidic environments was attained to be 1.2 ± 0.07 mol. The kinetics of the degradation reactions in both cases were the same, being unit order regarding [MnO_4^-], fewer than unit orders in [Flz], and fractional second orders in acid concentrations. The rate of oxidative degradation of fluconazole in H_2SO_4 was higher than that in $HClO_4$ at the same investigational circumstances. The addition of small amounts of Mg^{2+} and Zn^{2+} enhanced the degradation rates. The activation quantities were evaluated and debated. The gained oxidation products were characterized using spot tests. A mechanistic approach for the fluconazole degradation was suggested. Finally, the rate law expressions were derived which were agreed with the acquired outcomes. The rates of degradation for various [Flz] were mathematically modeled using the response surface methodology (RSM). The RSM model's conclusions and the experimental findings are in agreement. The oxidative degradation mechanism of Flz using density functional theory (DFT) was performed. The fluconazole drug degrades in acidic settings, protecting both the environment and human health, according to a method that is easy to use, powerful, inexpensive, practical, affordable, and safe.

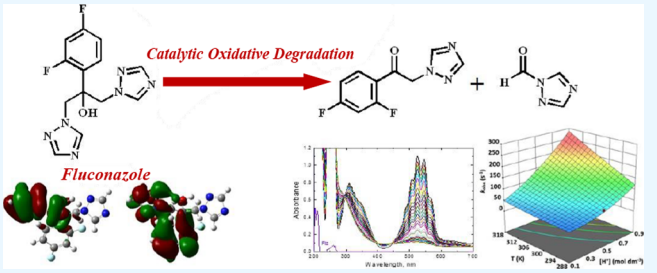

1. INTRODUCTION

The safe disposal of waste that is harmful to the environment is one of the most prominent challenges at the present time, especially with the technological and industrial development.[1−6] Medications or medical drugs are chemical substances used to detect, remedy, or avoid diseases in human, animals, and plants.[7−10] While medical drugs are fundamentally essential, they are foreign substances to the human body and must be eliminated after showing their medical role via the drug metabolism process in which drugs undergo a certain chemical reaction such as oxidation, reduction, hydrolysis, and so forth. Drug metabolism may transform drugs to medically effective, ineffective, or toxic materials that are excreted into the ecosystem and water sites.[11−13] Since the structures of these metabolites comprise complex organic compounds which can also stay in the environment for a long time without removal, these metabolites can be deliberated as dangerous pollutants.[14−16] Consequently, there is a huge interest to recognize efficient green treating methods or techniques for the removal or degradation of these materials to protect the ecosystem and human health.[17−20]

In various media, medical drugs are generally subjected to a variety of oxidation processes resulting in their decomposition or degradation.[21−25] Throughout these oxidation processes, oxidizers convert harmful or toxic materials to lower toxic ones which can be discharged safely to the environment.[26−30] Thus, oxidation of medical drugs has been considered as one of the supreme substantial methods for drug degradation and water-treating processes.[31] Fluconazole is a significant antifungal drug utilized for a wide number of fungal infections. Literature review illuminated very few reports that have been published on the oxidative degradation of fluconazole.[32] In these few reports, the employed strategies or chemicals may be relatively expensive or not widely available. In the light of these arguments, the existing investigation has been performed which is concerned with the study of kinetic and mechanistic features of oxidative

Received: September 15, 2023
Revised: January 30, 2024
Accepted: February 7, 2024
Published: February 22, 2024

degradation of the antibiotic fluconazole using the permanganate ion [MnO_4^-], which is one of the furthermost significant, available, powerful, inexpensive, and eco-friendly oxidants,[33,34] in a variety of acidic environments. The topmost aims of our investigation were to illuminate the capability of permanganate for the decomposition or degradation of fluconazole, to examine the impact of the acid type on the degradation kinetics as well as the influence of numerous effects. The catalytic impacts of certain metal cations, mainly Mg^{2+} and Zn^{2+}, were examined.[35] Also, the activation quantities were evaluated, and a reasonable degradation mechanism was suggested. Furthermore, this study is also extended to apply the RSM-CCD method to find the best answer through a sequence of well-planned tests. The individual and interaction effects of numerous conventional features were evaluated using CCD based on RSM in order to produce a more precise model for the sensitivity of the degradation rate of Flz. Additionally, the oxidative degradation mechanism of Flz using density functional theory (DFT) was performed. Accordingly, the present study aims to present a promising, simple, convenient, low-cost, and safe method for fluconazole disposal to protect the human health and ecosystem.

2. EXPERIMENTAL SECTION

2.1. Chemicals and Solutions. Fluconazole drug (Sigma-Aldrich, 98%) stock solution was made with DMSO solvent. A fresh potassium permanganate solution was made with bidistilled water. Stock solutions of H_2SO_4 and $HClO_4$ (Merck) were made by dilution of 99% H_2SO_4 and 70% $HClO_4$, respectively, with bidistilled water.[36] Solutions of sodium sulfate and sodium perchlorate (BDH, British Drug Houses) were prepared to fix the ionic strengths (I) in H_2SO_4 and $HClO_4$ environments, individually. Solutions of sulfate salts of magnesium and zinc (BDH) were utilized to catalyze the degradation rates.

2.2. Kinetic Measurements. The oxidative degradation reactions in both acidic environments were performed under pseudo-first-order circumstances ([Flz] ≫ [MnO_4^-]). The degradation reactions were tracked by recording the reduction of [MnO_4^-] absorbance at λ = 525 nm with time. The recorded UV−vis absorption readings were made on a thermostat Shimadzu UV−vis−NIR-3600 double-beam spectrophotometer. Most runs were performed three times to check the reproducibility (±4%).

2.3. Theoretical Calculation Analysis. The programs Gaussian View 06 and Gaussian 09W were used for all computations. The Lee−Yang−Parr (B3LYP) concept and the 6-31+G(d,p) base established were used to optimize the geometrical parameters of Flz, and also to calculate the Mulliken charge distribution.

2.4. Response Surface Methodology (RSM). Analyzing statistical information can help uncover hidden data and create models for prediction and estimation. Box and Wilson established the response surface methodology (RSM), a potent technique for analyzing and optimizing a phenomenon's interaction impacts.[37] In this case, the temperature (K), concentration of acid [H^+], and fluconazole dosage (mol dm^{-3}) are selected as independent factors, and the rate at which the drug degrades with the concentration of H2SO4 or HClO4 is selected as the response variable to be optimized via RSM. This decreased quantity of runs as well as the effectiveness of the modeling means that the face-centered composite design, or CCD for short, is used.[38] Thirty-six designs of experiment matrices and their outcomes are shown in Table 1.

Table 1. Experimental Designs Using Central Composite Design (CCD) for Degradation Rate

	operating conditions			response (10^3 k_{obs} (s^{-1}))	
run	10^2 [Flz] (mol dm^{-3})	[H^+] (mol dm^{-3})	T (K)	in sulfuric acid	in perchloric acid
1	2	0.5	288	15.6	9.0
2	2	0.5	298	19.8	15.1
3	2	0.5	308	26.3	21.8
4	2	0.5	318	33.0	24.6
5	4	0.5	288	28.1	20.7
6	4	0.5	298	39.1	24.9
7	4	0.5	308	49.0	37.9
8	4	0.5	318	64.4	47.8
9	6	0.5	288	36.2	29.4
10	6	0.5	298	53.9	40.6
11	6	0.5	308	72.3	50.1
12	6	0.5	318	94.8	74.8
13	8	0.5	288	50.8	34.1
14	8	0.5	298	66.8	50.4
15	8	0.5	308	92.7	66.4
16	8	0.5	318	120.9	89.9
17	10	0.5	288	61.3	42.3
18	10	0.5	298	80.2	58.1
19	10	0.5	308	110.1	85.0
20	10	0.5	318	140.8	115.3
21	6	0.1	288	2.7	1.8
22	6	0.1	298	3.2	2.3
23	6	0.1	308	4.5	2.9
24	6	0.1	318	5.6	7.2
25	6	0.3	288	14.0	12.0
26	6	0.3	298	20.2	15.0
27	6	0.3	308	27.1	20.8
28	6	0.3	318	37.5	29.8
29	6	0.7	288	58.8	53.8
30	6	0.7	298	93.0	69.9
31	6	0.7	308	127.0	97.7
32	6	0.7	318	163.0	119.7
33	6	0.9	288	99.1	78.2
34	6	0.9	298	133.4	112.5
35	6	0.9	308	196.9	138.5
36	6	0.9	318	241.8	201.3

3. RESULTS AND DISCUSSION

3.1. Reaction Stoichiometry and Product Description. Sets of reaction mixtures with various ratios of [MnO_4^-]/[Flz] at fixed [H^+] = 0.5 M and I = 1.0 M at 298 K were reacted for 24 h until the completion of degradation reactions. The unconsumed [MnO_4^-] was determined by spectrophotometry. The results designated that 4 mol of [MnO_4^-] was consumed to oxidize 5 mol of Flz to give the degradation products. The observed stoichiometry may be represented by the subsequent stoichiometric eq 1:

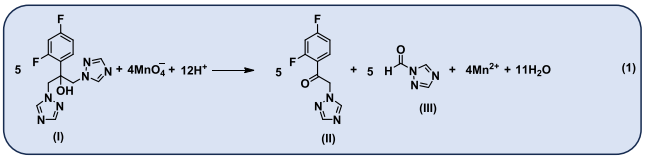

(1)

In eq 1, the compounds (I), (II), and (III) are Flz and its degradation products, individually. The products of fluconazole oxidation were separated by chromatography.[39] Then, the

https://doi.org/10.1021/acsomega.3c07074
ACS Omega 2024, 9, 10190−10200

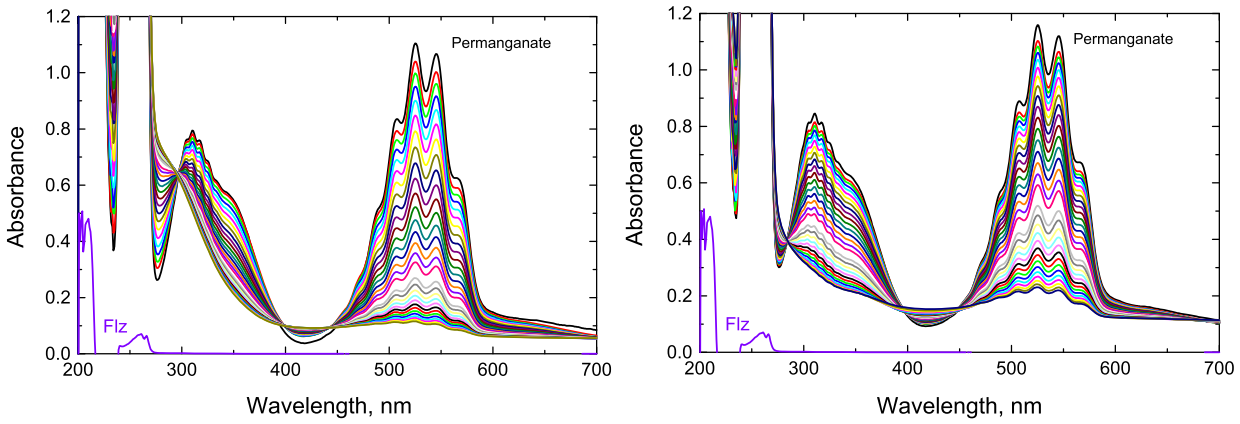

Figure 1. Spectroscopic changes during the permanganate oxidation of fluconazole (Flz) in (a) sulfuric acid and (b) perchloric acid environments. $[MnO_4^-] = 4.5 \times 10^{-4}$, $[Flz] = 1.0 \times 10^{-3}$, $[H^+] = 0.1$, and $I = 0.2$ mol dm^{-3} at 298 K. Scan time intervals = 1 min.

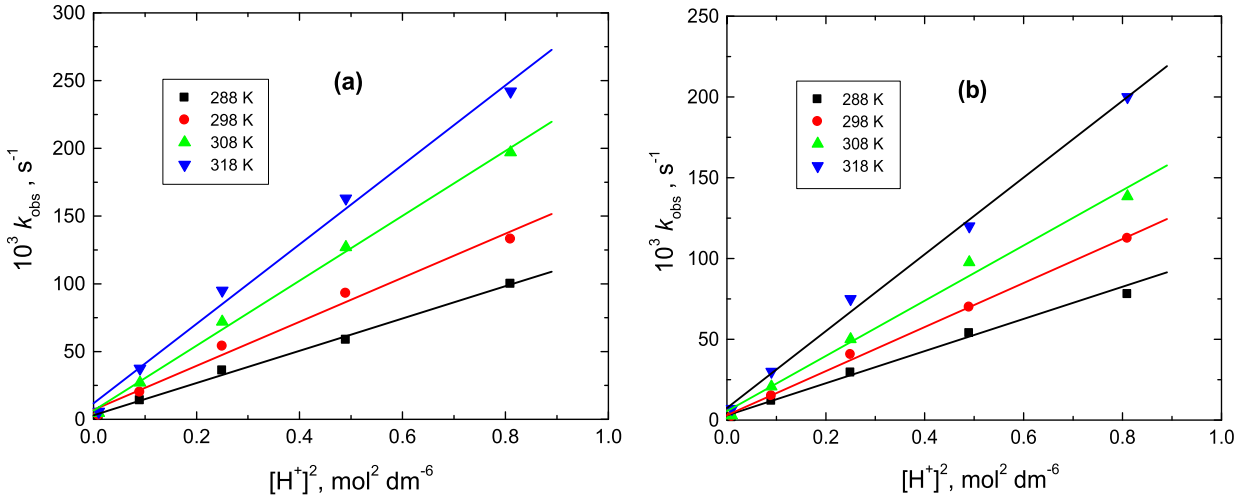

Figure 2. Plots of k_{obs} vs $[H^+]^2$ in the oxidative degradation of fluconazole in (a) sulfuric acid and (b) perchloric acid. $[MnO_4^-] = 4.5 \times 10^{-4}$, $[Flz] = 3.0 \times 10^{-2}$, and $I = 1.0$ mol dm^{-3} at 298 K.

separated products were recognized by spot tests via 2,4-dinitrophenylhydrazine, Schiff's, Tollen's and sodium nitroprusside reagents. It is widely known that the derivatives of 1,2,4-triazoles have a variety of biological functions. Based on earlier studies, most 1,2,4-triazole compounds appear to be relatively nontoxic. For example, Zhiyong Liu et al. estimated the toxicity of derivatives of 1,2,4-triazoles which demonstrated low toxicity and low environmental hazards.[40]

3.2. Spectroscopic Changes. Figure 1 shows the absorbance versus wavelength curves during the permanganate ion oxidation of fluconazole (Flz) in (a) sulfuric and (b) perchloric acid environments at 298 K. The figure illuminates the regular vanishing of permanganate ion band at $\lambda = 525$ nm. Figure 1 also shows no other features between 400 and 650 nm in which Mn^{IV} intermediate absorbs,[36] designating that manganese dioxide is not an oxidation product. Also, no increase in absorption at 418 nm was manifested, signifying that Mn^{IV} ions did not contribute to the oxidation process.

3.3. Order of Degradation Reactions Regarding their Constituents. The pseudo-first-order rate constants (k_{obs}) were estimated as the gradients of ln(absorbance) versus time plots (first-order plots). The orders of reactions with regard to [reactants] in both acidic environments were assessed from the gradients of log k_{obs} versus log(concentration) by varying [Flz] and $[H^+]$ in turn, whereas other constituents were retained fixed.

To investigate the dependence of the rates of oxidative degradation reactions on $[MnO_4^-]$ and hence the reaction order with regard to it, the preliminary $[MnO_4^-]$ was altered from 1×10^{-4} to 8×10^{-4} M at firm $[Flz] = 3.0 \times 10^{-2}$, $[H^+] = 0.5$, and $I = 1.0$ M at 298 K. It was noticed that the first-order graphs were approximately linear for the examined initial concentrations of $[MnO_4^-]$ (Figure S1 in the Supporting Information), signifying that the oxidative degradation reactions were of unit order in $[MnO_4^-]$. This result was indicated by the fixed values of k_{obs} in both acidic environments for various $[MnO_4^-]$ concentrations, as given in Table 1.

Also, in order to help in the elucidation of the degradation mechanism, the rates of degradation of fluconazole by $[MnO_4^-]$ was evaluated at various concentrations of the examined acidic environments (H_2SO_4 and $HClO_4$) at different temperatures. The gained outcomes signified increasing rates of antibiotic degradation with rising $[H^+]$, as shown from the values of k_{obs} listed in Table 1 (at 298 K) and in Table S1 in the Supporting Information at all temperatures. Plots of k_{obs} against $[H^+]$,[2] at different temperatures, were linear with + ve intercepts, as illustrated in Figure 2. In addition, the plots of log k_{obs} against log $[H^+]$ gave straight lines with gradients of 1.75 and 1.78, as shown in Figure S2 in the Supporting Information, signifying that these reactions were fractional second orders in $[H^+]$. On the other hand, the values of k_{obs} in both acidic environments were

https://doi.org/10.1021/acsomega.3c07074
ACS Omega 2024, 9, 10190−10200

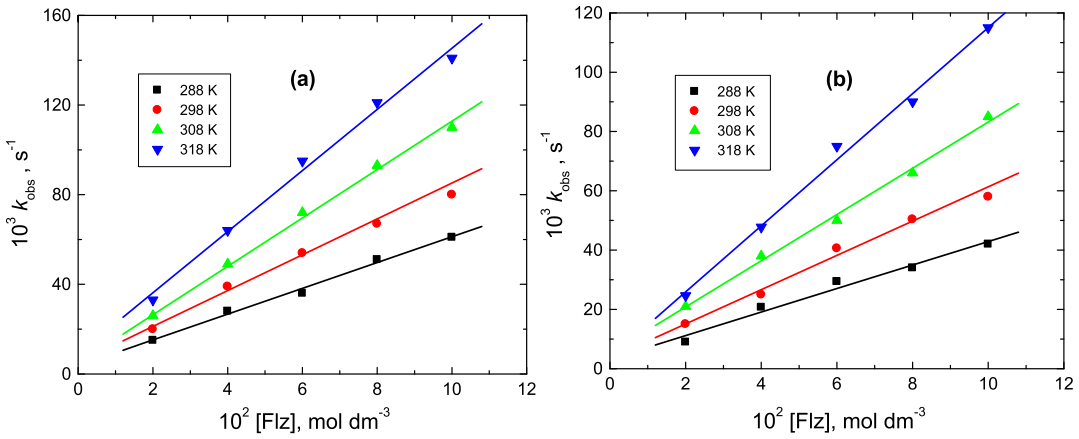

Figure 3. Plots of k_{obs} vs [Flz] in the oxidative degradation of fluconazole in (a) sulfuric acid and (b) perchloric acid. $[MnO_4^-] = 4.5 \times 10^{-4}$, $[H^+] = 0.5$, and $I = 1.0$ mol dm^{-3} at 298 K.

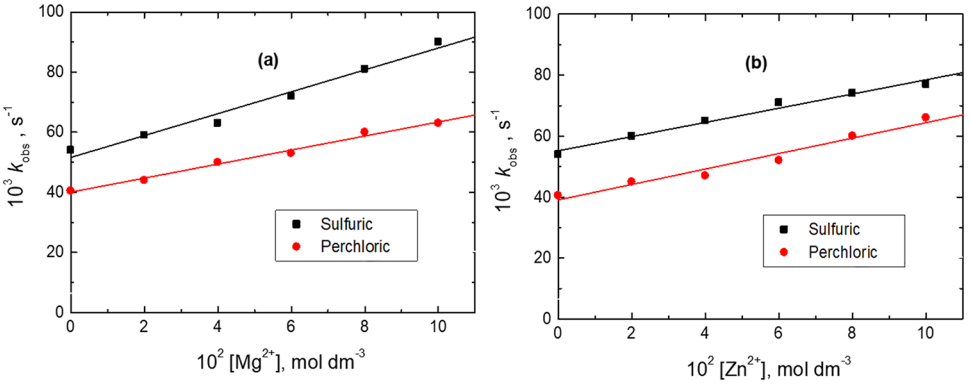

Figure 4. Influence of (a) $[Mg^{2+}]$ and $[Zn^{2+}]$ on the rates of the oxidative degradation of fluconazole by permanganate ion in sulfuric and perchloric acid environments. $[MnO_4^-] = 4.0 \times 10^{-4}$, [Flz] = 3.0×10^{-2}, $[H^+] = 0.5$, and $I = 1.0$ mol dm^{-3} at 298 K.

determined at several concentrations of fluconazole, [Flz], at stable $[MnO_4^-]$, $[H^+]$, *I*, and T. The acquired values of k_{obs} (presented in Tables 1 and S1) designated that the degradation rates were enhanced with rising [Flz]. In addition, the plots of k_{obs} versus [Flz] at different temperatures were straight with +ve intercepts (Figure 3). Furthermore, the plots of log [Flz] against log k_{obs} at 298 K gave straight lines with gradients of 0.86 and 0.88 in H_2SO_4 and $HClO_4$, correspondingly (Figure S3 in the Supporting Information), indicating that such degradation reactions were fractional first orders in fluconazole concentration.

3.4. Influences of the Ionic Strengths and Dielectric Constants of the Reaction Media. The kinetic runs were performed at numerous concentrations of sodium sulfate (in the case of H_2SO_4) and sodium perchlorate (in the case of $HClO_4$), while other ingredients persisted stable. The acquired results showed that the degradation rates were approximately unchanged as the value of ***I*** increased (Table 1). The influence of dielectric constants was examined by varying the acetic acid−water ratios in the reaction media, with all other circumstances being fixed. The experimental outcomes signified that the values of k_{obs} were altered unimportantly by increasing the acetic acid content in the reaction media (decreasing the dielectric constants).

3.5. Influence of Temperature on the Oxidative Degradation of Fluconazole. To investigate the impact of rising temperature on the degradation rates as well as to evaluate the activation parameters, kinetic experiments were carried out at various temperatures, namely 288, 298, 308, and 318 K, at numerous concentrations of fluconazole and acidic environments, but other variables remained constant. The experimental results (Figures 2, 3 and Tables 1, S1) showed that the degradation rates were set to improve by rising temperatures.

3.6. Influence of $[Mg^{2+}]$ and $[Zn^{2+}]$ on the Oxidative Degradation of Fluconazole. The catalytic impacts of certain environmentally friendly metal cations, namely Mg^{2+} and Zn^{2+}, on the degradation rates of fluconazole were studied in both acidic environments, and such rates were recorded after adding different concentrations of such cations at other fixed reaction ingredients. The obtained results (shown in Figure 4) indicated that the rates were improved by increasing the doses of the supplemented metal ions.

3.7. Acrylonitrile Test. To explore whether free radicals were formed throughout the examined degradation reactions or not, the acrylonitrile tests in both acidic environments were implemented. Acrylonitrile test was done by adding a certain volume of acrylonitrile to the reaction mixtures for 4 h. The investigational findings manifested that there were white precipitates formed, i.e., polymerization occurred in the reaction mixtures proposing the intervention of free radicals during such reactions.

3.8. Proposed Degradation Mechanism. The enhancement of the degradation rates by rising [H+] in addition to permanganate chemistry[41] recommends the construction of a more forceful oxidizing agent,

https://doi.org/10.1021/acsomega.3c07074
ACS Omega 2024, 9, 10190−10200

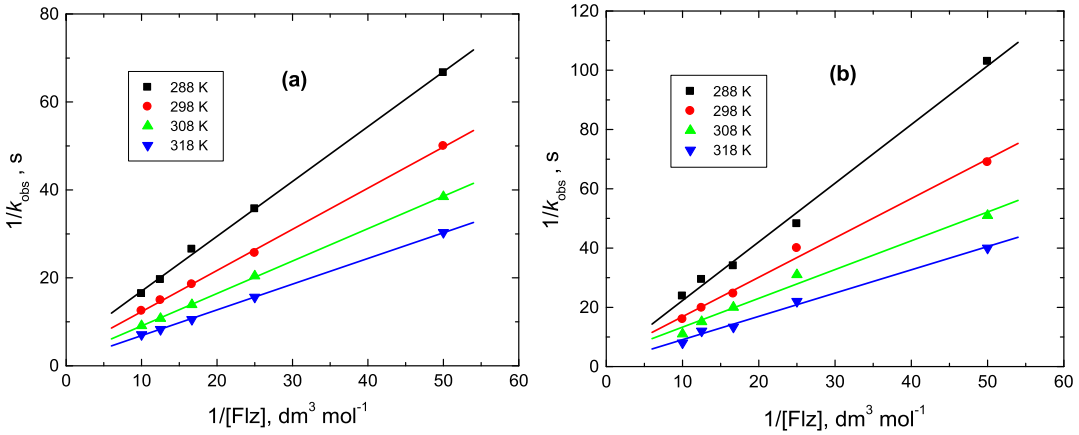

Figure 5. Plots of $1/k_{obs}$ vs $1/[Flz]$ in the oxidative degradation of fluconazole by permanganate ion in (a) sulfuric, and (b) perchloric acid environments at different temperatures. $[MnO_4^-] = 4 \times 10^{-4}$, $[H^+] = 0.5$, and $I = 1.0$ mol dm^{-3}.

$$Mn^{VII}O_4^- + H^+ \rightleftharpoons HMn^{VII}O_4 \quad (2)$$

The protonated permanganate ion ($HMnO_4$) is stronger than $[MnO_4^-]$ itself. Also, the fractional second-order reliance of the degradation rates regarding $[H^+]$ was an evidence of fluconazole protonation:

$$Flz + H^+ \rightleftharpoons [Flz - H]^+ \quad (3)$$

Thus, the protonated forms of both the oxidant and antibiotic were regarded as the reactive species in the rate-limiting stage of the degradation reactions.

On the other hand, the lower-than unit order reliance on fluconazole concentration consists with complex formation ($1/k_{obs}$ vs $1/[Flz]$ plot) (Figure 5). Furthermore, enhancing the rates with $[Mg^{2+}]$ and $[Zn^{2+}]$ signifies complexation between Flz and such cations.

In the light of these aspects, the plausible degradation mechanism involves the attack of the powerful acidic permanganate (produced through the reaction represented by eq 2) on the protonated fluconazole (produced through the reaction represented by eq 3) to construct a complex (C), as denoted by the succeeding equation,

$$Flz - H^+ + HMn^{VII}O_4 \rightleftharpoons [Flz - H - HMn^{VII}O_4]^+ (C) \quad (4)$$

The negligible impacts of both ionic strengths and dielectric constants of the reaction media propose that these reactions were among two neutral molecules or between an ion (Flz-H$^+$) and a neutral molecule ($HMn^{VII}O_4$).

The complex (C) is rapidly decomposed in the rate-limiting (slow) stage, leading to the formation of fluconazole free radical ($Flz^{\cdot+}$) and Mn^{VI} intermediate, as illustrated by eq 5,

$$[Flz - H - HMn^{VII}O_4]^+ (C) \rightarrow Flz^{\cdot+} + HMn^{VI}O_4^- + H^+ \quad (5)$$

The next step involves the attack of the formed $Flz^{\cdot+}$ by the Mn^{VI} intermediate to produce the final degradation products of fluconazole, eq 6,

$$Flz^{\cdot+} + HMn^{VI}O_4^- \rightarrow Flzoxidation\ products + HMn^{V}O_4^{2-} \quad (6)$$

The formed Mn^V species is very unstable in strong acidic environments, and it converted rapidly into Mn^{II} and Mn^{VII} by the disproportionation process as follows,

$$5HMn^{V}O_4^{2-} + 11H^+ \rightarrow 3Mn^{VII}O_4^- + 2Mn^{2+} + 3H_2O \quad (7)$$

This was followed by other fast steps between the permanganate ion and fluconazole, leading to the formation of the degradation products, as illuminated in the overall stoichiometric reaction 1.

3.9. Rate Law Equations. According to the proposed oxidative degradation mechanism and the rate-determining stage expressed by eq 5, the rate of vanishing of $[MnO_4^-]$ or construction of the complex (C) can be written by the succeeding rate equation,

$$\text{Rate} = \frac{-d[MnO_4^-]}{dt} = \frac{+d[C]}{dt} = k_1[C] \quad (8)$$

From reaction 2

$$K_1 = \frac{[HMnO_4]}{[MnO_4^-][H^+]},\ [HMnO_4] = K_1[MnO_4^-][H^+] \quad (9)$$

and from the reaction expressed by eq 3,

$$K_2 = \frac{[Flz^+]}{[Flz][H^+]},\ [Flz^+] = K_2[Flz][H^+] \quad (10)$$

$$K_3 = \frac{[C]}{[Flz^+][HMnO_4]},\ [C] = K_3[Flz^+][HMnO_4] \quad (11)$$

Exchanging eqs 9 and 10 into eq 11 gives,

$$[C] = K_1K_2K_3[Flz][MnO_4^-][H^+]^2 \quad (12)$$

Also exchanging eq 12 into eq 8 leads to,

$$\text{Rate} = k_1K_1K_2K_3[Flz][MnO_4^-][H^+]^2 \quad (13)$$

The total $[MnO_4^-]$ is given by (where "T" and 'F" stand for total and free):

$$[MnO_4^-]_T = [MnO_4^-]_F + [HMnO_4] + [C] \quad (14)$$

Exchanging eqs 9 and 11 into eq 14 results in,

$$[MnO_4^-]_T = [MnO_4^-]_F + K_1[MnO_4^-]_F[H^+] + K_1K_2K_3[MnO_4^-]_F[Flz][H^+]^2 \quad (15)$$

https://doi.org/10.1021/acsomega.3c07074
ACS Omega 2024, 9, 10190−10200

Table 2. Dependence of the Values of k_{obs} on $[MnO_4^-]$, [Flz], $[H^+]$, and Ionic Strength (I) in the Oxidative Degradation of Fluconazole by Permanganate Ion in Sulfuric and Perchloric Acid Environments at 298 K

10^4 $[MnO_4^-]$ (mol dm^{-3})	10^2 [Flz] (mol dm^{-3})	$[H^+]$ (mol dm^{-3})	I (mol dm^{-3})	10^3 k_{obs} (s^{-1}) sulfuric acid	10^4 $[MnO_4^-]$ (mol dm^{-3}) perchloric acid
1.0	6.0	0.5	1.0	52.1	40.9
2.0	6.0	0.5	1.0	53.7	42.1
4.0	6.0	0.5	1.0	53.9	40.6
6.0	6.0	0.5	1.0	52.4	41.0
8.0	6.0	0.5	1.0	54.2	39.8
4.0	2.0	0.5	1.0	19.8	15.1
4.0	4.0	0.5	1.0	39.1	24.9
4.0	6.0	0.5	1.0	53.9	40.6
4.0	8.0	0.5	1.0	67.0	50.4
4.0	10.0	0.5	1.0	79.9	58.0
4.0	6.0	0.1	1.0	3.2	2.3
4.0	6.0	0.3	1.0	20.2	15.0
4.0	6.0	0.5	1.0	53.9	40.6
4.0	6.0	0.7	1.0	93.0	69.9
4.0	6.0	0.9	1.0	133.4	112.5
4.0	6.0	0.5	1.0	53.9	40.6
4.0	6.0	0.5	1.5	52.4	41.2
4.0	6.0	0.5	2.0	53.1	40.5
4.0	6.0	0.5	2.5	52.7	41.6
4.0	6.0	0.5	3.0	54.2	40.1

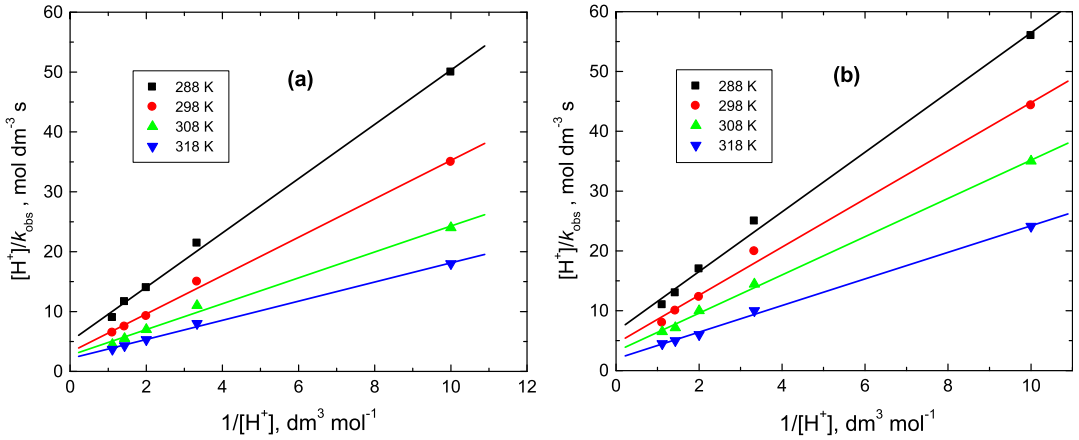

Figure 6. Plots of $[H^+]/k_{obs}$ vs $1/[H^+]$ in the oxidative degradation of fluconazole by permanganate ion in (a) sulfuric acid and (b) perchloric acid environments at different temperatures. $[MnO_4^-] = 4 \times 10^{-4}$, [Flz] = 6.0×10^{-2}, and I = 1.0 mol dm^{-3}.

$$[MnO_4^-]_T = [MnO_4^-]_F(1 + K_1[H^+] + K_1K_2K_3[Flz][H^+]^2) \quad (16)$$

Consequently,

$$[MnO_4^-]_F = \frac{[MnO_4^-]_T}{1 + K_1[H^+] + K_1K_2K_3[Flz][H^+]^2} \quad (17)$$

As a result of high $[H^+]$, we can propose that,

$$[H^+]_T = [H^+]_F \quad (18)$$

Correspondingly,

$$[Flz]_T = [Flz]_F \quad (19)$$

Replacement of eqs 17−19 into eq 13 (and excluding "T' and 'F" subscripts) results in,

$$\text{Rate} = \frac{k_1K_1K_2K_3[MnO_4^-][Flz][H^+]^2}{1 + K_1[H^+] + K_1K_2K_3[Flz][H^+]^2} \quad (20)$$

Under pseudo-first-order circumstance, the rate law can be stated by the equation,

$$\text{Rate} = \frac{-d[MnO_4^-]}{dt} = k_{obs}[MnO_4^-] \quad (21)$$

Comparing eqs 20 and 21,

$$k_{obs} = \frac{k_1K_1K_2K_3[Flz][H^+]^2}{1 + K_1[H^+] + K_1K_2K_3[Flz][H^+]^2} \quad (22)$$

and

$$\frac{1}{k_{obs}} = \left(\frac{1 + K_1[H^+]}{k_1K_1K_2K_3[H^+]^2}\right)\frac{1}{[Flz]} + \frac{1}{k_1} \quad (23)$$

https://doi.org/10.1021/acsomega.3c07074
ACS Omega 2024, 9, 10190−10200

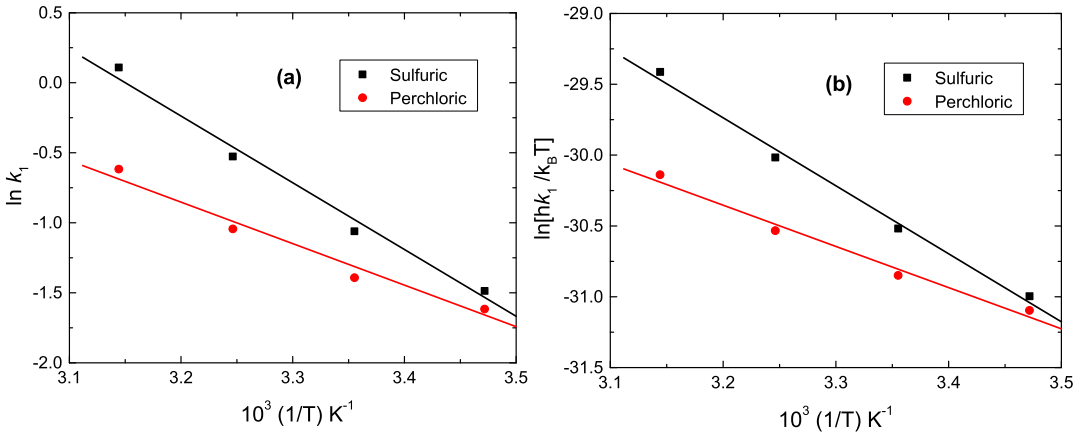

Figure 7. (a) Arrhenius, and (b) Eyring plots of k_1 in the oxidative degradation of fluconazole (Flz) by permanganate ion in (a) sulfuric and (b) perchloric acid environments. $[MnO_4^-] = 5.0 \times 10^{-4}$, $[Flz] = 5.0 \times 10^{-2}$, $[H^+] = 0.5$, and $I = 1.0$ mol dm^{-3}.

Rendering to eq 23, the graphs of $1/k_{obs}$ versus $1/[Flz]$ at fixed $[H^+]$ should be linear with +ve intercepts, as were manifested from Figure 5 at different temperatures. The values of the rate constant of the rate-limiting stage, k_1, at various temperatures are evaluated and presented in Table 2.

The acquired insignificant intercepts (in Figure 5) may lead to shorten eq 23 to 24:

$$\frac{[H^+]}{k_{obs}} = \left(\frac{1}{k_1K_1K_2K_3[Flz]}\right)\frac{1}{[H^+]} + \frac{1}{k_1K_2K_3[Flz]} \quad (24)$$

According to eq 24, when the graphs were made between $[Flz]/k_{obs}$ and $1/[H^+]$, good straight lines with + ve intercepts would be obtained, as illustrated in Figure 6, which approve the legality of the proposed mechanism.

3.10. Activation Parameters. The activation quantities related to the rate-limiting stage, k_1, were evaluated via Arrhenius and Eyring equations (illustrated in Figures 7a,b, correspondingly). The acquired values of activation quantities, namely, entropy ($\Delta S‡$), enthalpy ($\Delta H‡$), free energy ($\Delta G‡$), and activation energy ($E_a‡$) are listed in Table 3. The acquired

Table 3. Activation Parameters of k_1 in the Oxidative Degradation of Fluconazole by Permanganate Ion in Sulfuric and Perchloric Acid Environments[a]

acidic medium	$\Delta S‡$ (J mol^{-1} K^{-1})	$\Delta H‡$ (kJ mol^{-1})	$\Delta G‡$ (kJ mol^{-1})	$E_a‡$ (kJ mol^{-1})
Sulfuric	−118.89	39.82	75.25	39.57
Perchloric	−174.59	24.11	76.14	24.61

[a] $[MnO_4^-] = 4 \times 10^{-4}$ and $I = 1.0$ mol dm^{-3}.

great negative $\Delta S‡$ values verify the compression of the constructed intermediate complex (C). Also, the positive $\Delta H‡$ and $\Delta G‡$ values designated the endothermic construction of the complex and its nonspontaneity, individually.[42]

3.11. Mechanism of Oxidative Degradation with Assistance from DFT Calculations. The electrostatic potential (ESP) is a useful descriptor for distinguishing the locations of electrophilic (areas with low electron density) and nucleophilic (areas with high electron density) reactions because of its link to electron density. Blue is connected with the electrophilic region, while red is related with the nucleophilic region (which is quickly damaged by oxidants).[43−46] The carbons at the linker between the benzene and the two triazole rings were related with the electrophilic blue region in Figure 8a, while the nitrogen atoms of the two triazole rings were the site of the nucleophilic red region. The frontier-orbital theory states that nucleophilic interaction more likely occurs at particles with higher values of the lowest unoccupied molecular orbital (LUMO), and electrophilic interaction is more likely to happen at particles with higher values of the highest occupied molecular orbital (HOMO).[47−49] According to certain experts, atoms with higher frontier electron density HOMO values are more susceptible to oxidation.[50−52] Figure 8b gives the Mulliken charge distributions for each atom. C1 in the benzene ring of the Flz structure had the highest HOMO value, which was 0.408, followed by C3 in the benzene ring and C17 and C22 in the triazole ring, which had HOMO values of 0.354 and 0.0322, respectively. C19 was one of the positions, with the HOMO value greater than 0.2. According to Figure 8c,d, the border electron densities of HOMO and LUMO for Flz were individually estimated.

3.12. RSM Model Optimization. From the investigational data in Table 1, a semiempirical appearance equation that comprised 10 statistically substantial factors was obtained and stated as follows:

$$Y_1 = 61.7 + 37.3A + 82.7B + 30.0C + 0AB + 16.1AC + 37.0BC - 2.4A^2 + 22.0B^2 + 3.3C^2 \quad (25)$$

$$Y_2 = 44.6 + 28.5A + 64.8B + 23.7C + 0AB + 14.2AC + 27.7BC - 1.2A^2 + 20.6B^2 + 5.1C^2 \quad (26)$$

where Y_1 and Y_2 are the response variables of k_{obs} in the presence of H_2SO_4 and $HClO_4$, respectively. A, B, and C represent three experimental factors, the fluconazole drug concentration (mol dm^{-3}), acid concentration $[H^+]$, and temperature (K), respectively. With a good correlation (R^2 = 0.994 376 and 0.991 for Y_1 and Y_2, respectively), the comparison of experimental values (Y_{exp}) in 374 that are consistent with the responses predicted by the typical (Y_{cal}) 375 for the deterioration rate indicates that this is generally 377. As shown in Figure 9, this makes the investigative series very clear.

Afterward, the variance among the values of the results from experimentation and estimates (residuals) could be pragmatic to assess the perfect suitability. The externally estimated residual design is specified in Figure 10. All residuals may be shown to be uniformly distributed within a line that is straight, suggesting

https://doi.org/10.1021/acsomega.3c07074
ACS Omega 2024, 9, 10190−10200

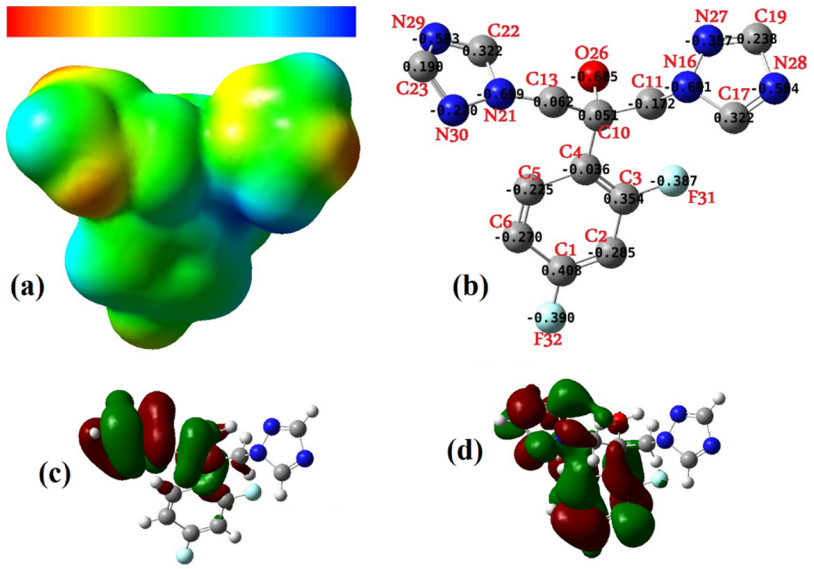

Figure 8. Theoretical calculation of the Flz structure; (a) electrostatic potential (ESP), (b) Mulliken charge distributions, and (c,d) HOMO and LUMO.

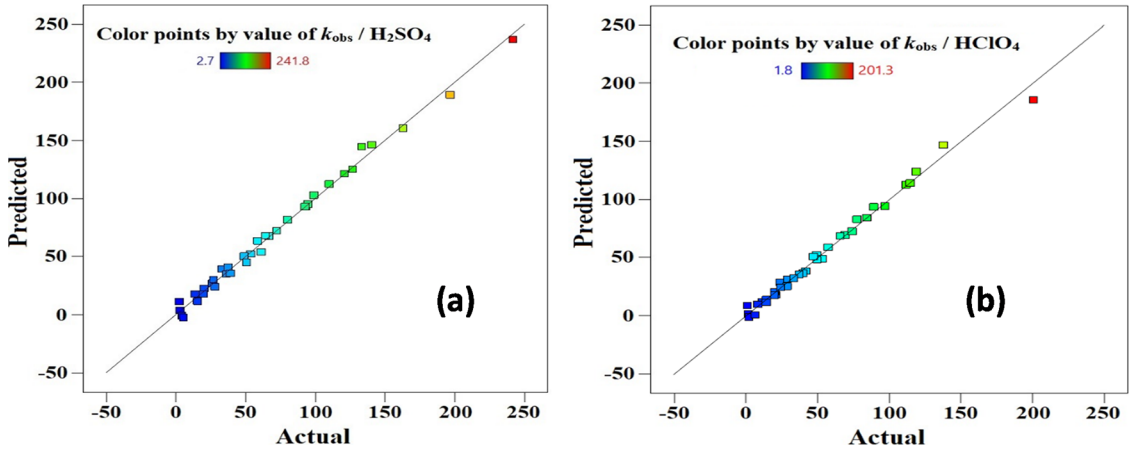

Figure 9. Experimental and calculated values for the degradation rate of Flz in (a) H_2SO_4 and (b) $HClO_4$.

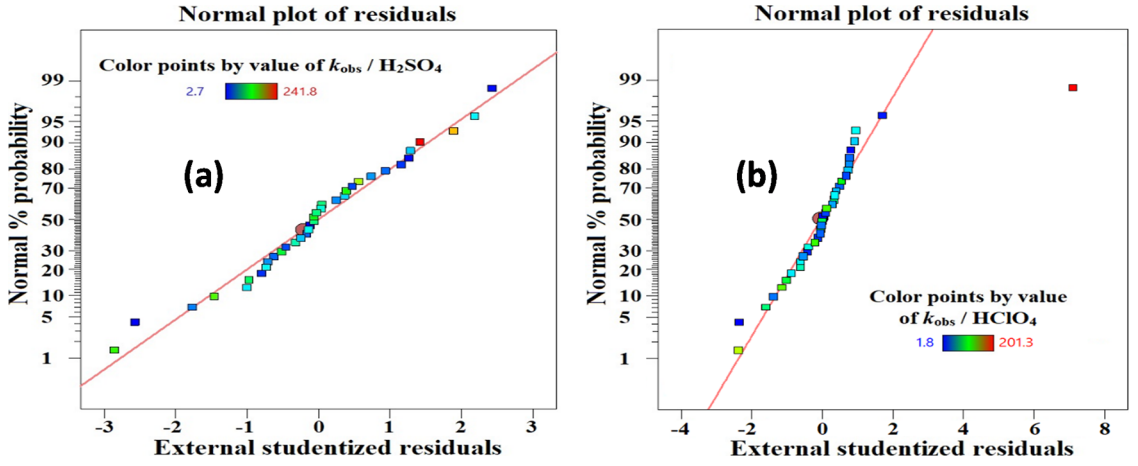

Figure 10. Externally studentized residual plot in the presence of (a) H_2SO_4 and (b) $HClO_4$.

there is is no serious non-normality. Based on these findings, the residuals appeared to be caused by random scatter, and the model developed is appropriate for describing the link between the deterioration rate and the three aforementioned factors.

The values of P (significant probability values) on the other hand confirm that the model terms are highly significant[53−56] if they are smaller than 0.05. In addition, Figure 11 demonstrates that, regardless of how the expected value varies, in addition, the

https://doi.org/10.1021/acsomega.3c07074
ACS Omega 2024, 9, 10190−10200

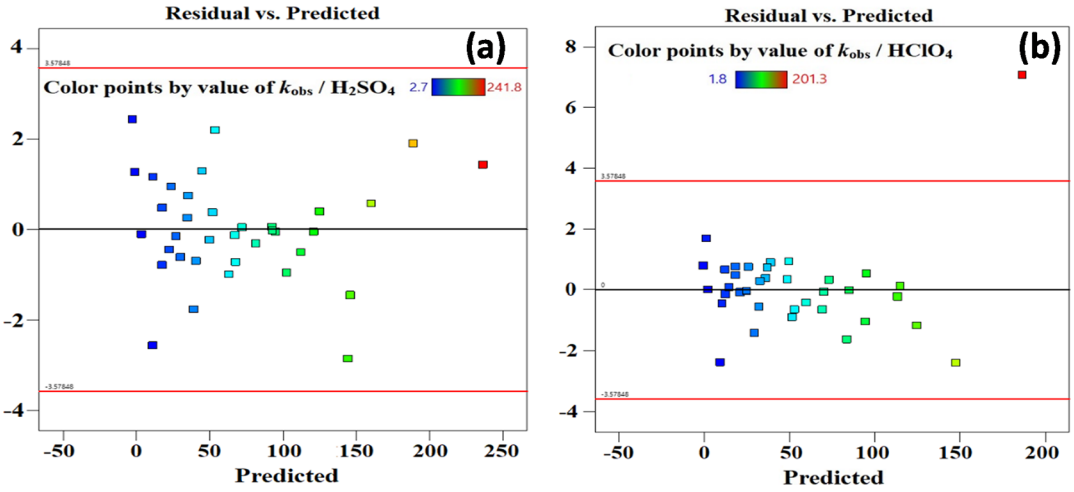

Figure 11. Residuals vs predicted in (a) H_2SO_4 and (b) $HClO_4$.

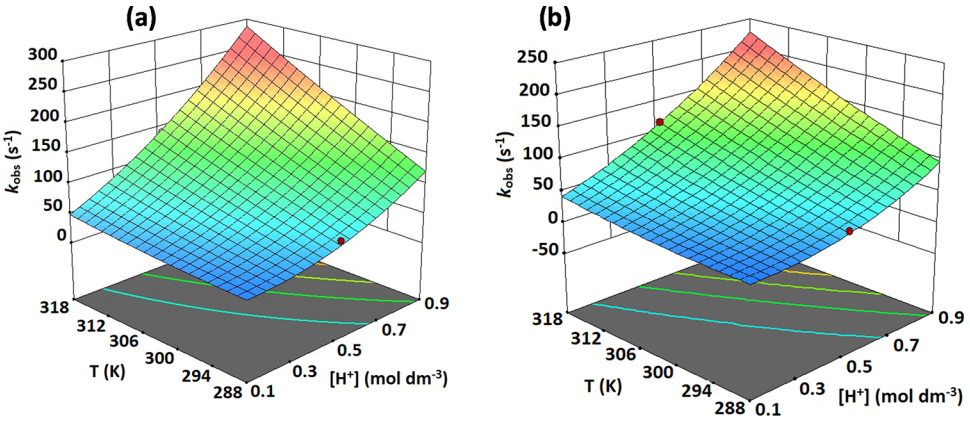

Figure 12. Three-dimensonal surface plots: effect of $[H^+]$ × temperature (T) on the degradation of Flz in (a) H_2SO_4 and (b) $HClO_4$.

residuals lack any discernible pattern or systematic organization and are distributed between −4 and +4.

These results lead to the conclusion that the created model is enough to describe the link between the deteriorating efficiency and the previously indicated parameters, and the residuals approximate an arbitrary scatter.[57] The results are shown in Figure 12, which shows that the degradation rate of Flz increases by rising the temperature and increasing the acid concentration $[H^+]$ of both sulfuric and perchloric acids. The closeness of the two results suggests that the semiempirical expression is sufficient to maximize Flz degradation.

4. CONCLUSIONS

Oxidative degradation of Flz was discovered kinetically using permanganate ion in H_2SO_4 and $HClO_4$ electrolytes at various temperatures. The degradation reactions were found to be acid-catalyzed. The rate of oxidative degradation of fluconazole in H_2SO_4 electrolyte was higher than that in $HClO_4$ electrolyte at the same investigational circumstances. Addition of little amounts of Mg^{2+} and Zn^{2+} enhanced the degradation rates. The activation quantities of the mechanism at slow stage were calculated and debated. The obtained oxidation products were characterized using spot tests. A mechanistic approach for the fluconazole degradation was suggested. The rate law expressions were derived which agreed with the acquired outcomes. Mulliken charge distributions indicated that C1 in the benzene ring of the Flz structure had the highest HOMO value, which was 0.408, followed by C3 in the benzene ring and C17 and C22 in the triazole ring, which had HOMO values of 0.354 and 0.0322, respectively. The present research work may introduce a promising, modest, opportune, low-priced, and harmless tool to be employed for dilapidation of fluconazole in acid atmospheres to defend the humanoid healthiness and ecosystems.

■ ASSOCIATED CONTENT

Supporting Information

The Supporting Information is available free of charge at https://pubs.acs.org/doi/10.1021/acsomega.3c07074.

Identified separated products of degradation reactions; effect of temperature on k_{obs} ($\times 10^{-3}$ s^{-1}) in the oxidative degradation of fluconazole by permanganate ion in sulfuric and perchloric acid environments; plots of ln *a*bsorbance vs time in the oxidative degradation of fluconazole by permanganate ion; plots of log k_{obs} vs log $[H^+]$ in the oxidative degradation of fluconazole by permanganate ion; and plots of log k_{obs} vs log [Flz] in the oxidative degradation of fluconazole by permanganate ion (PDF)

■ AUTHOR INFORMATION

Corresponding Authors

Arafat Toghan − *Chemistry Department, College of Science, Imam Mohammad Ibn Saud Islamic University (IMSIU),*

https://doi.org/10.1021/acsomega.3c07074
ACS Omega 2024, 9, 10190−10200

Riyadh 11623, Saudi Arabia; Chemistry Department, Faculty of Science, South Valley University, Qena 83523, Egypt; orcid.org/0000-0002-1423-1147; Email: arafat.toghan@yahoo.com, aatahmed@imamu.edu.sa

Ahmed Fawzy − *Chemistry Department, Faculty of Science, Assiut University, Assiut 71516, Egypt*; Email: afsaad13@yahoo.com

Ahmed A. Farag − *Egyptian Petroleum Research Institute (EPRI), Nasr City 11727 Cairo, Egypt;* orcid.org/0000-0002-9019-5635; Email: ahmedafm@yahoo.com, ahmedafm2023@outlook.com

Authors

Nada Alqarni − *Department of Chemistry, College of Sciences and Arts in Balgarn, University of Bisha, Bisha 61922, Saudi Arabia*

Ahmed M. Eldesoky − *Department of Chemistry, University College in Al-Qunfudhah, Umm Al-Qura University, Makkah 21912, Saudi Arabia*

Omar K. Alduaij − *Chemistry Department, College of Science, Imam Mohammad Ibn Saud Islamic University (IMSIU), Riyadh 11623, Saudi Arabia*

Complete contact information is available at: https://pubs.acs.org/10.1021/acsomega.3c07074

Notes

The authors declare no competing financial interest.

■ ACKNOWLEDGMENTS

The authors extend their appreciation to the Deanship of Scientific Research at Imam Mohammad Ibn Saud Islamic University (IMSIU) for funding and supporting this work through Research Partnership Program no.RP-21-09-74.

■ REFERENCES

(1) Mary, H.; Acharya, S. S.; Padmanaban, S.; Pandian, S. *Chapter 1 - Challenges and Opportunities Associated with Different Forms of Waste Resources Utilizations*; Selvasembian, R.; Wan Azelee, N. I.; Shanmugam, S. R.; Venkatachalam, P.; Mishra, A. K. B. T.-V. of W. for S. D., Eds.; Elsevier, 2023; pp 3−32. DOI: 10.1016/B978-0-323-95417-4.00001-9.

(2) Fawzy, A.; Al Bahir, A.; Alqarni, N.; Toghan, A.; Khider, M.; Ibrahim, I. M.; Abulreesh, H. H.; Elbanna, K. Evaluation of Synthesized Biosurfactants as Promising Corrosion Inhibitors and Alternative Antibacterial and Antidermatophytes Agents. *Sci. Rep.* **2023**, *13* (1), 2585.

(3) Alamro, F. S.; Mostafa, A. M.; Abu Al-Ola, K. A. A.; Ahmed, H. A.; Toghan, A. Synthesis of Ag Nanoparticles-Decorated CNTs via Laser Ablation Method for the Enhancement the Photocatalytic Removal of Naphthalene from Water. *Nanomaterials* **2021**, *11* (8), 2142.

(4) Alamro, F. S.; Mostafa, A. M.; Ahmed, H. A.; Toghan, A. Zinc Oxide/Carbon Nanotubes Nanocomposite: Synthesis, Characterization and Catalytic Reduction of 4-Nitrophenol via Laser Assistant Method. *Surfaces and Interfaces* **2021**, *26*, No. 101406.

(5) Toghan, A.; Abd El-Lateef, H. M.; Taha, K. K.; Modwi, A. Mesoporous TiO2@g-C3N4 Composite: Construction, Characterization, and Boosting Indigo Carmine Dye Destruction. *Diam. Relat. Mater.* **2021**, *118*, No. 108491.

(6) Toghan, A.; Modwi, A. Boosting Unprecedented Indigo Carmine Dye Photodegradation via Mesoporous MgO@g-C3N4 Nanocomposite. *J. Photochem. Photobiol. A Chem.* **2021**, *419*, No. 113467.

(7) Farag, A. A.; Migahed, M. A.; Al-Sabagh, A. M. Adsorption and Inhibition Behavior of a Novel Schiff Base on Carbon Steel Corrosion in Acid Media. *Egypt. J. Pet.* **2015**, *24* (3), 307−315.

(8) Assaf, H. F.; Salah, H.; Hashem, N.; Khodari, M.; Toghan, A. Fabrication of an Electrochemical Sensor Based on Copper Waste Wire Recycling and Its Application. *Sensors Actuators A Phys.* **2021**, *331*, No. 112962.

(9) Altowyan, A. S.; Toghan, A.; Ahmed, H. A.; Pashameah, R. A.; Mwafy, E. A.; Alrefaee, S. H.; Mostafa, A. M. Removal of Methylene Blue Dye from Aqueous Solution Using Carbon Nanotubes Decorated by Nickel Oxide Nanoparticles via Pulsed Laser Ablation Method. *Radiat. Phys. Chem.* **2022**, *198*, No. 110268.

(10) Alrebdi, T. A.; Ahmed, H. A.; Alsubhe, E.; Alkallas, F. H.; Mwafy, E. A.; Adel Pashameah, R.; Toghan, A.; Mostafa, A. M. Synthesis of NiO-PVA Nanocomposite by Laser Assisted-Method and Its Characterization as a Novel Adsorbent for Removal Phosphate from Aqueous Water. *Opt. Laser Technol.* **2022**, *156*, No. 108526.

(11) Mohamed, H. A.; Farag, A. A.; Badran, B. M. Corrosion Inhibitiob of Mild Steel Using Emulsified Thiazole Adduct in Different Binder Systems. *Eurasian Chem. J.* **2008**, *10* (1), 67−77.

(12) Fawzy, A. Silver-Catalyzed Oxidation of Atropine Drug by Cerium(IV) in Aqueous Perchlorate Solutions: A Kinetics and Mechanistic Approach. *J. Drug Des. Med. Chem.* **2016**, *2* (5), 51.

(13) Fawzy, A. Oxidative Degradation of Atropine Drug by Permanganate Ion in Perchloric and Sulfuric Acid Solutions: A Comparative Kinetic Study. *Adv. Biochem.* **2016**, *4* (5), 58.

(14) Bongomin, F.; Oladele, R. O.; Gago, S.; Moore, C. B.; Richardson, M. D. A Systematic Review of Fluconazole Resistance in Clinical Isolates of Cryptococcus Species. *Mycoses* **2018**, *61* (5), 290−297.

(15) Fawzy, A. Removal of Toxic Tellurium (IV) Compounds via Bioreduction Using Flucloxacillin in Aqueous Acidic Medium: A Kinetic and Mechanistic Approach. *J. Mol. Liq.* **2019**, *292*, No. 111436.

(16) Fawzy, A.; Abdallah, M.; Alqarni, N. Oxidative Degradation of Neomycin and Streptomycin by Cerium(IV) in Sulphuric and Perchloric Acid Solutions. *J. Mol. Liq.* **2020**, *312*, No. 113439.

(17) Peng, X.; Ou, W.; Wang, C.; Wang, Z.; Huang, Q.; Jin, J.; Tan, J. Occurrence and Ecological Potential of Pharmaceuticals and Personal Care Products in Groundwater and Reservoirs in the Vicinity of Municipal Landfills in China. *Sci. Total Environ.* **2014**, *490*, 889−898.

(18) Fawzy, A.; Abdallah, M.; Alqarni, N. Degradation of Ampicillin and Flucloxacillin Antibiotics via Oxidation by Alkaline Hexacyanoferrate(III): Kinetics and Mechanistic Aspects. *Ind. Eng. Chem. Res.* **2020**, *59* (37), 16217−16224.

(19) Fawzy, A.; Solo, O.; Morad, M. Oxidation of Barbituric and Thiobarbituric Acids by Chromium Trioxide in Different Acidic Media: A Kinetic and Mechanistic Aspects. *J. Mol. Struct.* **2021**, *1229*, No. 129495.

(20) Fawzy, A.; El Guesmi, N.; Althagafi, I. I.; Asghar, B. H. A Study of the Kinetics and Mechanism of Chromic Acid Oxidation of Isosorbide, a Chiral Biomass-Derived Substratein Aqueous Perchlorate Solution. *Transition Met. Chem.* **2017**, *42* (3), 229−236.

(21) Kabel, K. I.; Farag, A. A.; Elnaggar, E. M.; Al-Gamal, A. G. Removal of Oxidation Fragments from Multi-Walled Carbon Nanotubes Oxide Using High and Low Concentrations of Sodium Hydroxide. *Arab. J. Sci. Eng.* **2015**, *41*, 2211.

(22) Kabel, K. I.; Farag, A. A.; Elnaggar, E. M.; Al-Gamal, A. G. Improvement of Graphene Oxide Characteristics Depending on Base Washing. *J. Superhard Mater.* **2015**, *37* (5), No. 050056.

(23) Toghan, A.; Gadow, H. S.; Fawzy, A.; Alhussain, H.; Salah, H. Adsorption Mechanism, Kinetics, Thermodynamics, and Anticorrosion Performance of a New Thiophene Derivative for C-Steel in a 1.0 M HCl: Experimental and Computational Approaches. *Metals (Basel).* **2023**, *13* (9), 1565.

(24) Dardeer, H. M.; Toghan, A. A Novel Route for the Synthesis of Pseudopolyrotaxane Containing γ-Cyclodextrin Based on Environmental Waste Recycling. *J. Mol. Struct.* **2021**, *1227*, No. 129707.

(25) Toghan, A.; Taha, K. K.; Modwi, A. TiO2−ZnO Composites Fabricated via Sonication Assisted with Gelatin for Potential Use in Rhodamine B Degradation. *J. Mater. Sci. Mater. Electron.* **2021**, *32* (2), 2471−2485.

(26) Fawzy, A.; Abdallah, M.; Alqarni, N. Mechanistic and Thermodynamic Aspects of Oxidative Removal of Flucloxacillin by Different Oxidants in an Acidic Medium. *J. Mol. Liq.* **2021**, *325*, No. 115160.
(27) Altalhi, A. A.; Mohammed, E. A.; Morsy, S. S. M.; Negm, N. A.; Farag, A. A. Catalyzed Production of Different Grade Biofuels Using Metal Ions Modified Activated Carbon of Cellulosic Wastes. *Fuel* **2021**, *295*, No. 120646.
(28) Amer, A.; Sayed, G. H.; Ramadan, R. M.; Rabie, A. M.; Negm, N. A.; Farag, A. A.; Mohammed, E. A. Assessment of 3-Amino-1H-1,2,4-Triazole Modified Layered Double Hydroxide in Effective Remediation of Heavy Metal Ions from Aqueous Environment. *J. Mol. Liq.* **2021**, *341*, No. 116935.
(29) Fawzy, A.; Alsharief, H. H.; Toghan, A.; Al Bahir, A.; Alhasani, M.; Alqarni, N.; Alsaedi, A. M. R.; Fargaly, T. A. Evaluation of Protection Performances of Novel Synthesized Bis-Oxindole-Based Derivatives for the Corrosion of Aluminum in Acidic Environment. *J. Mol. Struct.* **2023**, *1294*, No. 136443.
(30) Fawzy, A.; Toghan, A. Inhibition Evaluation of Chromotrope Dyes for the Corrosion of Mild Steel in an Acidic Environment: Thermodynamic and Kinetic Aspects. *ACS Omega* **2021**, *6* (5), 4051−4061.
(31) Fawzy, A.; Toghan, A. Unprecedented Treatment Strategy of Aquatic Environments: Oxidative Degradation of Penicillin G by Chromium Trioxide in Acidic Media and the Impact of Metal Ion Catalysts: Kinetics and Mechanistic Insights. *ACS Omega* **2020**, *5* (50), 32781−32791.
(32) Fawzy, A.; Alqarni, N.; El-Gammal, B.; Toghan, A.; Hassan, N. A.; Algarni, Z. Auspicious water treatment approach. Oxidative degradation of fluconazole and voriconazole antibiotics by CrO_3 in different acidic environments: Kinetics, mechanistic and thermodynamic modelling. *J. Saudi Chem. Soc.* **2022**, *26*, No. 101396.
(33) Fawzy, A.; Ashour, S. S.; Musleh, M. A. Kinetics and Mechanism of Oxidation of Histidine by Permanganate Ions in Sulfuric Acid Medium. *Int. J. Chem. Kinet.* **2014**, *46* (7), 370−381.
(34) Fawzy, A.; Shaaban, M. R. Kinetic and Mechanistic Investigations on the Oxidation of N'-Heteroaryl Unsymmetrical Formamidines by Permanganate in Aqueous Alkaline Medium. *Transit. Met. Chem.* **2014**, *39* (4), 379−386.
(35) Abdel Wahab, M. M.; Sayed, G. H.; Ramadan, R. M.; Mady, A. H.; Rabie, A. M.; Farag, A. A.; Negm, N. A.; Mohamed, E. A. Synergistic Effects of Graphene Oxide Grafted with Barbituric Acid Nanocomposite for Removal of Heavy Metals from Aqueous Solution. *Nanotechnol. Environ. Eng.* **2023**, *8*, 347.
(36) Stewart, R. *Oxidation in Organic Chemistry, Part A*; Academic Press: New York, 1965.
(37) Box, G. E. P.; Wilson, K. On the Experimental Attainment of Optimum Conditions. *J. R. Stat. Soc.* **1951**, *13*, 1−45.
(38) Montgomery, D. C. *Design and Analysis of Experiments*, 10th ed.; John Wiley & Sons, 2017.
(39) Rendina, A. R.; Cleland, W. W. Separation of Aldehydes and Ketones by Chromatography on Dowex-50 in the Ethylenediamine Form. *Anal. Biochem.* **1981**, *117* (1), 213−218.
(40) Liu, Z.; Dang, K.; Gao, J.; Fan, P.; Li, C.; Wang, H.; Li, H.; Deng, X.; Gao, Y.; Qian, A. Toxicity Prediction of 1,2,4-Triazoles Compounds by QSTR and Interspecies QSTTR Models. *Ecotoxicol. Environ. Saf.* **2022**, *242*, No. 113839.
(41) Carrington, A.; Symons, M. C. R. Structure and Reactivity of the Oxyanions of Transition Metals. *Chem. Rev.* **1963**, *63* (5), 443−460.
(42) Freeman, F.; Fuselier, C. O.; Armstead, C. R.; Dalton, C. E.; Davidson, P. A.; Karchesfski, E. M.; Krochman, D. E.; Johnson, M. N.; Jones, N. K. Permanganate Ion Oxidations.13. Soluble Manganese(IV) Species in the Oxidation of 2,4(1H,3H)-Pyrimidinediones (Uracils). *J. Am. Chem. Soc.* **1981**, *103* (5), 1154−1159.
(43) Farag, A. A.; Eid, A. M.; Shaban, M. M.; Mohamed, E. A.; Raju, G. Integrated Modeling, Surface, Electrochemical, and Biocidal Investigations of Novel Benzothiazoles as Corrosion Inhibitors for Shale Formation Well Stimulation. *J. Mol. Liq.* **2021**, *336*, No. 116315.
(44) Farag, A. A. Oil-in-Water Emulsion of a Heterocyclic Adduct as a Novel Inhibitor of API X52 Steel Corrosion in Acidic Solution. *Corros. Rev.* **2018**, *36* (6), 575−588.
(45) Farag, A. A.; Badr, E. A. Non-Ionic Surfactant Loaded on Gel Capsules to Protect Downhole Tubes from Produced Water in Acidizing Oil Wells. *Corros. Rev.* **2020**, *38* (2), 151−164.
(46) Shaban, S. M.; Badr, E. A.; Shenashen, M. A.; Farag, A. A. Fabrication and Characterization of Encapsulated Gemini Cationic Surfactant as Anticorrosion Material for Carbon Steel Protection in Down-Hole Pipelines. *Environ. Technol. Innov.* **2021**, *23*, No. 101603.
(47) Farag, A. A.; Abdallah, H. E.; Badr, E. A.; Mohamed, E. A.; Ali, A. I.; El-Etre, A. Y. The Inhibition Performance of Morpholinium Derivatives on Corrosion Behavior of Carbon Steel in the Acidized Formation Water: Theoretical, Experimental and Biocidal Evaluations. *J. Mol. Liq.* **2021**, *341*, No. 117348.
(48) Shaban, M. M.; Negm, N. A.; Farag, R. K.; Fadda, A. A.; Gomaa, A. E.; Farag, A. A.; Migahed, M. A. Anti-Corrosion, Antiscalant and Anti-Microbial Performance of Some Synthesized Trimeric Cationic Imidazolium Salts in Oilfield Applications. *J. Mol. Liq.* **2022**, *351*, No. 118610.
(49) Hashem, H. E.; Farag, A. A.; Mohamed, E. A.; Azmy, E. M. Experimental and Theoretical Assessment of Benzopyran Compounds as Inhibitors to Steel Corrosion in Aggressive Acid Solution. *J. Mol. Struct.* **2022**, *1249*, No. 131641.
(50) Mohamed, E. A.; Hashem, H. E.; Azmy, E. M.; Negm, N. A.; Farag, A. A. Synthesis, Structural Analysis, and Inhibition Approach of Novel Eco-Friendly Chalcone Derivatives on API X65 Steel Corrosion in Acidic Media Assessment with DFT & MD Studies. *Environ. Technol. Innov.* **2021**, *24*, No. 101966.
(51) Toghan, A.; Fawzy, A.; Al Bahir, A.; Alqarni, N.; Sanad, M. M. S.; Khairy, M.; Alakhras, A. I.; Farag, A. A. Computational Foretelling and Experimental Implementation of the Performance of Polyacrylic Acid and Polyacrylamide Polymers as Eco-Friendly Corrosion Inhibitors for Copper in Nitric Acid. *Polymers (Basel).* **2022**, *14* (22), 4802.
(52) Toghan, A.; Fawzy, A.; Alakhras, A. I.; Farag, A. A. Electrochemical and Theoretical Examination of Some Imine Compounds as Corrosion Inhibitors for Carbon Steel in Oil Wells Formation Water. *Int. J. Electrochem. Sci.* **2022**, *17*, 2212108.
(53) Fawzy, A.; Alduaij, O. K.; Al-Bahir, A.; Alshammari, D. A.; Alqarni, N.; Eldesoky, A. M.; Farag, A. A.; Toghan, A. A Comparative Study of Pyridine and Pyrimidine Derivatives Based Formamidine for Copper Corrosion Inhibition in Nitric Acid: Experimental and Computational Exploration. *Int. J. Electrochem. Sci.* **2024**, *19*, No. 100403.
(54) Al-Sabagh, A. M.; Abdou, M. I.; Migahed, M. A.; Fadl, A. M.; Farag, A. A.; Mohammedy, M. M.; Abd-Elwanees, S.; Deiab, A. Influence of Ilmenite Ore Particles as Pigment on the Anticorrosion and Mechanical Performance Properties of Polyamine Cured Epoxy for Internal Coating of Gas Transmission Pipelines. *Egypt. J. Pet.* **2018**, *27* (4), 427−436.
(55) Toghan, A.; Gouda, M. H.; Zahran, H. F.; Alakhras, A. I.; Sanad, M. M. S.; Elessawy, N. A. Development of a New Promising Nanocomposite Photocatalyst of Polyaniline/Carboxylated Graphene Oxide Supported on PVA Film to Remove Different Ecological Pollutants. *Diam. Relat. Mater.* **2023**, *139*, No. 110400.
(56) Fawzy, A.; Toghan, A. Unprecedented Treatment Strategy of Aquatic Environments: Oxidative Degradation of Penicillin G by Chromium Trioxide in Acidic Media and the Impact of Metal Ion Catalysts: Kinetics and Mechanistic Insights. *ACS Omega* **2020**, *5* (50), 32781−32791.
(57) Toghan, A.; Fawzy, A.; Alakhras, A. I.; Alqarni, N.; Zaki, M. E. A.; Sanad, M. M. S.; Farag, A. A. Experimental Exploration, RSM Modeling, and DFT/MD Simulations of the Anticorrosion Performance of Naturally Occurring Amygdalin and Raffinose for Aluminum in NaOH Solution. *Coatings* **2023**, *13* (4), 704.

https://doi.org/10.1021/acsomega.3c07074
ACS Omega 2024, 9, 10190−10200